FGFR2b signaling regulates ex vivo submandibular gland epithelial cell proliferation and branching morphogenesis

Zachary Steinberg[1], Christopher Myers[1], Vernon M. Heim[1], Colin A. Lathrop[1], Ivan T. Rebustini[1], Julian S. Stewart[1], Melinda Larsen[1,2] and Matthew P. Hoffman[1,*]

[1]Matrix and Morphogenesis Unit, Craniofacial Developmental Biology and Regeneration Branch, National Institute of Dental and Craniofacial Research, National Institutes of Health, 30 Convent Drive, MSC 4370, Bethesda, MD 20892-4370, USA
[2]Developmental Mechanisms Section, Craniofacial Developmental Biology and Regeneration Branch, National Institute of Dental and Craniofacial Research, National Institutes of Health, 30 Convent Drive, MSC 4370, Bethesda, MD 20892-4370, USA
*Author for correspondence (e-mail: mhoffman@mail.nih.gov)

Accepted 22 December 2004

Development 132, 1223-1234
Published by The Company of Biologists 2005
doi:10.1242/dev.01690

Summary

Branching morphogenesis of mouse submandibular glands is regulated by multiple growth factors. Here, we report that ex vivo branching of intact submandibular glands decreases when either *FGFR2* expression is downregulated or soluble recombinant FGFR2b competes out the endogenous growth factors. However, a combination of neutralizing antibodies to FGF1, FGF7 and FGF10 is required to inhibit branching in the intact gland, suggesting that multiple FGF isoforms are required for branching. Exogenous FGFs added to submandibular epithelial rudiments cultured without mesenchyme induce distinct morphologies. FGF7 induces epithelial budding, whereas FGF10 induces duct elongation, and both are inhibited by FGFR or ERK1/2 signaling inhibitors. However, a PI3-kinase inhibitor also decreases FGF7-mediated epithelial budding, suggesting that multiple signaling pathways exist. We immunolocalized FGF receptors and analyzed changes in *FGFR*, *FGF* and *MMP* gene expression to identify the mechanisms of FGF-mediated morphogenesis. FGFR1b and FGFR2b are present throughout the epithelium, although FGFR1b is more highly expressed around the periphery of the buds and the duct tips. FGF7 signaling increases *FGFR1b* and *FGF1* expression, and MMP2 activity, when compared with FGF10, resulting in increased cell proliferation and expansion of the epithelial bud, whereas FGF10 stimulates localized proliferation at the tip of the duct. FGF7- and FGF10-mediated morphogenesis is inhibited by an MMP inhibitor and a neutralizing antibody to FGF1, suggesting that both FGF1 and MMPs are essential downstream mediators of epithelial morphogenesis. Taken together, our data suggests that FGFR2b signaling involves a regulatory network of *FGFR1b*/*FGF1*/*MMP2* expression that mediates budding and duct elongation during branching morphogenesis.

Key words: Fibroblast growth factor receptors, FGF7, FGF10, Signaling, Salivary gland development, Organ culture

Introduction

Fibroblast growth factors (FGFs), a family of 23 growth factors, are crucial for many developmental processes, including branching morphogenesis (Martin, 1998; Ornitz, 2000). Multiple FGF and FGF receptor (FGFR) isoforms are expressed in the developing mouse submandibular gland (SMG) (Hoffman et al., 2002). Altered SMG phenotypes occur in some FGF/FGFR transgenic mice (Ornitz and Itoh, 2001). The FGF10-null mouse has an absence of salivary, thyroid and pituitary glands, with minor defects in the formation of teeth, kidneys, hair follicles and digestive organs (Min et al., 1998; Ohuchi et al., 2000; Sekine et al., 1999). The FGFR2b-null mouse (De Moerlooze et al., 2000) and the soluble-FGFR2 transgenic mouse (Celli et al., 1998) do not develop salivary glands. The FGF7-null mouse has defects in kidney and hair development (Guo et al., 1996; Qiao et al., 1999); however, no SMG phenotype was reported. Functional compensation by other FGFs may occur with a single-FGF knockout. Targeted overexpression of FGF7 with the K14 promoter caused smaller salivary glands, excessive salivation, and a delay in gland differentiation (Guo et al., 1993). FGF8-conditional mutant and FGF8-hypomorphic mice also have defects in SMG development and differentiation (Jaskoll et al., 2004). Taken together, these studies suggest a primary role for FGF10/FGFR2b signaling in the initiation of the gland, an essential role for FGF8 at later stages, and possibly a role for FGF7 during differentiation. However, little is known about the role of FGFs after SMG initiation during early branching morphogenesis.

Branching morphogenesis of ex vivo SMGs involves both FGFR signaling (Hoffman et al., 2002; Jaskoll et al., 2002; Morita and Nogawa, 1999) and EGFR signaling (Kashimata and Gresik, 1997; Kashimata et al., 2000). Previously, we identified a role for FGFR1 and phosphatidylinositol 3-kinase (PI3K) in SMG branching morphogenesis (Larsen et al., 2003). Here, we investigate the role of FGF7 and FGF10 signaling through FGFR2b. The known ligands for FGFR2b are FGF1, FGF3, FGF7 and FGF10. FGF7 and FGF10 both bind with

high affinity to FGFR2b (Yeh et al., 2003), although FGF10 also binds FGFR1b (Igarashi et al., 1998).

Matrix metalloproteinases (MMPs) regulate branching morphogenesis in many organ systems. During ureteric bud branching, growth factors and extracellular matrix (ECM) components modulate MMP expression (Pohl et al., 2000). In mammary epithelium, interplay between MMPs, growth factors and morphogens is necessary for branching, although the MMPs are not required for proliferation (Simian et al., 2001). In SMG organ culture, exogenous collagenase decreased cleft formation, and TIMP1 increased it, by regulating collagen III fibril formation at the cleft site (Hayakawa et al., 1992; Nakanishi et al., 1986). However, the role of MMPs in SMG morphogenesis may not only be to cleave the collagen matrix, but also to release FGF-binding heparan sulfates from proteoglycans, or to directly cleave FGFRs to regulate FGFR function (Powers et al., 2000). MMP2 cleaves the extracellular domain of FGFR1, resulting in a cleavage product that can still bind FGFs and may regulate FGF signaling (Levi et al., 1996).

A fundamental but complex question is how FGFs interact with multiple FGFRs and result in distinct downstream signaling that coordinates proliferation, migration, differentiation and, ultimately, morphogenesis. Here, we investigate the role of FGFR2b and its ligands in serum-free ex vivo submandibular gland organ culture. We used salivary epithelium, separated from mesenchyme, to define distinct morphogenetic roles for FGF7 and FGF10. The downstream signaling and gene expression is ERK1/2-dependent and involves a regulatory network of *FGFR1b/FGF1/MMP2* expression. FGF7 and FGF10 cause localized cell proliferation and they require both FGF1 and MMP activity to regulate epithelial budding and duct elongation during branching morphogenesis.

Materials and methods

Ex vivo submandibular gland organ culture

Submandibular/sublingual salivary gland rudiments (referred to as SMGs) dissected from either E12 or E13 ICR mice were cultured on Whatman Nuclepore Track-etch filters (13 mm, 0.1 μm pore size; VWR, Buffalo Grove, IL) at the air/medium interface. The filters were floated on 200 μl of DMEM/F12 in 50-mm glass-bottom microwell dishes (MatTek, Ashland, MA). The medium was supplemented with 100 U/ml penicillin, 100 μg/ml streptomycin, 150 μg/ml vitamin C and 50 μg/ml transferrin. Five gland rudiments were cultured on each filter at 37°C in a humidified 5% CO_2/95% air atmosphere. Glands were photographed at 2, 20 and 44 hours, and the end buds were counted at each timepoint. Each experiment was repeated at least three times.

Mesenchyme-free epithelia were cultured as previously described (Morita and Nogawa, 1999), with some modifications. E13 glands were incubated in 1.6 U/ml of Dispase in Hanks' balanced salt solution (Roche Molecular Biochemicals, Indianapolis, IN) at 37°C for 20 minutes. Epithelia with up to five buds were separated from the mesenchyme with fine forceps in Hanks' solution containing 10% BSA. Most importantly, horse serum was omitted from the media. The epithelial rudiments were placed on a Nuclepore filter, covered with 15 μl of laminin-1 (1 mg/ml; Trevigen, Gaithersburg, MD) or growth factor-reduced Matrigel, diluted 1:1 in medium (5 mg/ml; BD Biosciences, San Jose, CA), and the filter was floated on top of 200 μl of medium as described above. FGFs were added either alone or in combination to the media, and the glands were cultured for up to 44 hours. FGF1 (1, 20, 100, 500 ng/ml), FGF2 (1,10, 100, 200 ng/ml), FGF3 (1, 10, 100, 1000 ng/ml), FGF7 (50, 100, 500, 1000 ng/ml), or FGF10 (200, 500, 1000, 2000 ng/ml), alone or in combination, was added to the cultures (all growth factors were purchased from R&D Systems, Minneapolis, MN).

Antisense experiments

Antisense and sense oligonucleotides were minimally phosphorothioated as previously described (Uhlmann et al., 2000). Residues that were phosphorothioate-modified are shown in bold: KGFR sense (1372-1390), 3′-**ca**gg**c**caa**c**cag**tc**tg**cc**t-5′; KGFR antisense (1390-1372), 3′-**ag**g**c**aga**c**tgg**t**tgg**cct**g-5′ (Post et al., 1996); Bek antisense (first two residues modified for mouse), 3′-**tg**g**c**agaa**c**tg**t**c**aa**c-5′; Bek sense, 3′-**gt**tga**c**ag**ttc**tg**cc**a-5′; antisense to both KGFR/Bek, 5′-**gc**tga**cc**a**t**gg**tca**c-3′; sense to both KGFR/Bek, 5′**gt**ga**cc**a**t**gg**t**c**ag**c-3′ (Post et al., 1996). Oligonucleotides (2 μM) were added to the media and replaced after 44 hours. RT-PCR was used to determine the decrease in gene expression. FITC-labeled oligonucleotide uptake was detected with confocal microscopy (data not shown) [similar to Hoffman et al. (Hoffman et al., 2002)].

Addition of recombinant FGFRs and FGF antibodies

E12 or E13 SMGs were cultured for 48 hours as described above with recombinant (r) FGFRs or neutralizing antibodies to FGFs. The human rFGFR1b and rFGFR1c, and mouse rFGFR2b, rFGFR2c and rFGFR3c, chimeras were all added alone (1-20 μg/ml) and in various combinations (R&D Systems, Minneapolis, MN). Neutralizing antibodies to FGF1 (AF232), FGF2 (AF233), FGF7 (MAB251) and Mouse IgG (MAB002) (R&D Systems), an FGF10 antibody previously used for neutralization of FGF10 activity (sc7375-L) (Harada et al., 2002), and a goat IgG control (sc2028-L; Santa Cruz Biotechnology) were added to the culture medium at concentrations of 10, 25 and 50 μg/ml. Combinations of either two or three anti-FGF antibodies (25 μg/ml each) were also tested. Glands were cultured for 44 hours, and branching morphogenesis was quantitated as described above.

Time-lapse microscopy

SMGs or epithelial rudiments in laminin-1 were prepared as described above and incubated in an environmental chamber fitted on a Zeiss SV25 inverted microscope. Images were acquired once every 20 minutes for 36 hours using MetaMorph Software (Universal Imaging, Dowingtown, PA) and assembled into movies.

Whole-mount immunofluorescence

Proliferation and apoptosis were detected as previously described (Hoffman et al., 2002), using a BrdU Labeling and Detection Kit and an In Situ Cell Death Detection Kit, TMR-red (Roche Molecular Biochemicals, Indianapolis, IN), as described in the manufacturer's instructions. Nuclei were stained with SYBR-green, and for immunostaining, mouse-on-mouse reagents were used (M.O.M. reagents; Dako, Carpenteria, CA). With the apoptosis kit, the epithelium was stained with FITC-peanut lectin (Vector Laboratories, Burlingame, CA). The BrdU and apoptosis staining were quantitated using MetaMorph Software. The fluorescent pixels from all optical sections were measured and expressed as a ratio of the total pixel area of the gland or BrdU:SYBR-green. Five glands/condition were used, and the experiments were repeated three times.

Epithelial glands or rudiments cultured in laminin were also fixed on the filters in 4% paraformaldehyde (PFA) for 1 hour, permeabilized with 0.1% Triton X-100 for 15 minutes, and blocked overnight with 10% donkey serum, M.O.M. blocking reagent, and 1% BSA. Primary antibodies were added in M.O.M. protein reagent for 3 hours at room temperature and secondary reagents were added in PBS-Tween 20 (0.1%) for 2 hours. Primary antibodies included Flg (sc-121), bek (sc-122) (Santa Cruz), E-cadherin Mab 36 (BD Biosciences, Pharmingen), MMP2-hinge and MMP9-hinge (Triple Point

Diagnostics), alpha-6 integrin (GoH3, Chemicon), and perlecan (MAB1948, Chemicon). Secondary antibodies were all donkey F(ab)2 fragments labeled with Cy2, Cy3 and Cy5 (Jackson Immunoresearch Laboratories, West Grove, PA). All images were obtained with a Zeiss LSM 510 confocal microscope.

Rescue of rFGFR2b treatment with exogenous FGFs

E13 salivary gland rudiments were cultured with 1.6 μg/ml rFGFR2b, the concentration required to give ~50% inhibition of branching (data not shown). All FGFs tested were added at the same time as the rFGFR2b at the beginning of the experiment. A range of doses was tested, but only a single dose is shown. FGF1 (20, 100, 500, 1000 ng/ml), FGF3 (100, 500, 1000 ng/ml), FGF7 (50, 100, 500, 1000 ng/ml), FGF10 (100, 500, 1000, 2500 ng/ml), FGF2 (10, 100, 500, 1000 ng/ml), FGF4 (10, 100, 500, 1000 ng/ml) and BMP7 (10, 100, 500, 1000 ng/ml) were added to the cultures.

Inhibition of FGF-induced epithelial morphogenesis

Epithelial rudiments were dissected free of mesenchyme and cultured in laminin-1 gels. The growth factors, inhibitors and rFGFRs were added at the same time. DMSO or PBS with 0.1% BSA was used as a carrier control. Su5402 (1, 2.5, 5, 10 μM) was a gift from Dr F. Unda (Universidad del Pais Vasco, Spain). LY294002 (5 and 10 μM), UO126 (5 and 10 μM) and GO6983 (1.5 μM) were all from Calbiochem (La Jolla, CA). The rudiments were cultured for 44 hours and photographed, and the bud number and duct length were measured using MetaMorph Software.

Gelatin zymography of epithelium-conditioned media

The media were concentrated in centrifugal filters (Millipore Biomax 10K NMWL Membrane, 0.5 ml volume). Glands were lysed, and total protein quantitated (BCA Assay, Pierce). The volume of media concentrate was normalized to protein in the gland lysates and analyzed on a 10% gelatin zymogram gel developed using Invitrogen Zymogram Buffers (Invitrogen, Carlsbad, CA). HT1080-conditioned medium (Chemicon, Temecula, CA) was included as a positive control.

Real-time PCR

At least eight epithelial rudiments were cultured in 15 μl of laminin-1 as described above. DNase-free RNA was prepared using an RNAqueous-4 PCR kit and a DNA-free DNase removal reagent (Ambion, Austin, TX). TaqManTM reverse transcription reagents (Applied Biosystems, Foster City, CA) were used to make cDNA. Real-time PCR was performed using primers designed with similar properties using Beacon Designer Software (Biorad, Hercules, CA), SYBR-green PCR Master Mix (Applied Biosystems), and a Biorad MyIQ real-time PCR thermocycler. Each cDNA (5-10 ng) was amplified with an initial denaturation at 95°C for 10 minutes, then 95°C for 15 seconds and 68°C for 30 seconds, for 40 cycles. Gene expression was normalized to the housekeeping gene *S29*. Melt-curve analysis was routinely run, and the PCR reactions were also analyzed by gel electrophoresis to confirm that a single product of the expected size was amplified. The reactions were run in triplicate, repeated three times, and the results combined to generate the graphs.

Results

Perturbation of FGFR2 function decreases ex vivo branching morphogenesis of SMGs

We used two approaches to perturb FGFR2 function. First, *FGFR2* expression was downregulated in E12 SMGs with antisense oligonucleotides that have been previously shown to decrease FGFR levels (Post et al., 1996; Zang et al., 2003). Branching was decreased ~66% when compared with either the control oligonucleotide or the KGFR/Bek sense oligonucleotide control (Fig. 1A,B). A ~50% decrease in *FGFR2* expression was measured by RT-PCR after 24 hours (Fig. 1C), when compared with control and sense oligonucleotide-treated glands. The glands appeared to cleft, yet normal bud expansion did not occur, which suggests FGFR2 is important during ex vivo branching morphogenesis.

Second, we perturbed FGFR function by adding soluble rFGFR isoforms to the media, to compete out the endogenous FGFs. We tested a range of concentrations of FGFR isoforms, but rFGFR2b had the most dramatic effect on branching morphogenesis (Fig. 2A). The epithelium was smaller than the control and lacked enlarged terminal buds, but formed elongated ducts. The phenotype of the rFGFR2b-treated glands reflected how many buds were present at the beginning of the experiment. Smaller glands, 3-5 buds, were more strongly inhibited (see Fig. 2B and Movie 1 in supplementary material). Lumen formation occurred within the ducts and is apparent in the light microscope images in the main ducts (Fig. 2A,C). rFGFR1b- and rFGFR3c-treated glands had fewer buds overall, but the morphology was similar to that of the control. Combinations of rFGFR1b and rFGFR3c had additive effects (data not shown), but the inhibition was less than with rFGFR2b (Fig. 2B). Our results suggest that multiple FGFs are involved in branching, that the ligands for FGFR2b play an important role in bud formation and expansion, and that other FGFs may regulate the extent of branching.

FGFR2b regulates epithelial cell proliferation in salivary gland organ culture

Proliferation was measured by BrdU incorporation, and FGFR2 was immunolocalized to the terminal epithelial buds of control and rFGFR2b-treated glands (Fig. 3A,B). rFGFR2b

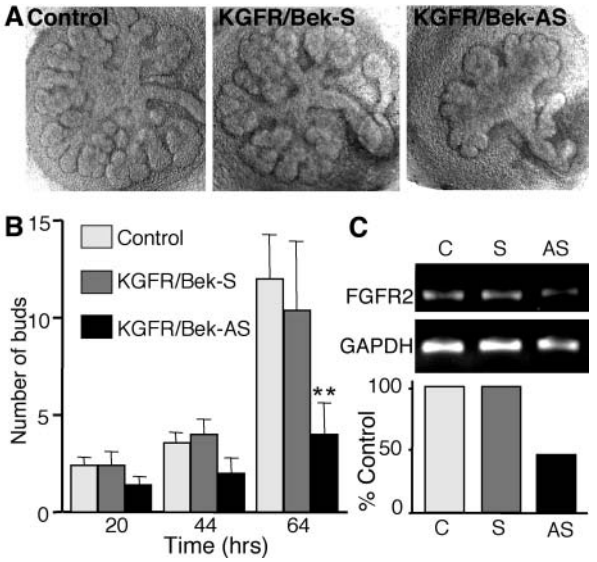

Fig. 1. (A) Antisense oligonucleotides to KGFR/Bek decrease branching morphogenesis of E12 SMGs; a representative photograph of each group is shown. (B) The number of terminal buds of at least six glands at each timepoint was counted. There was a significant decrease (ANOVA, $^{**}P<0.01$) in the number of buds in the antisense-treated glands. (C) Antisense oligonucleotides decrease *FGFR2* expression by ~50%; the expression of *FGFR2* was normalized to *GAPH*.

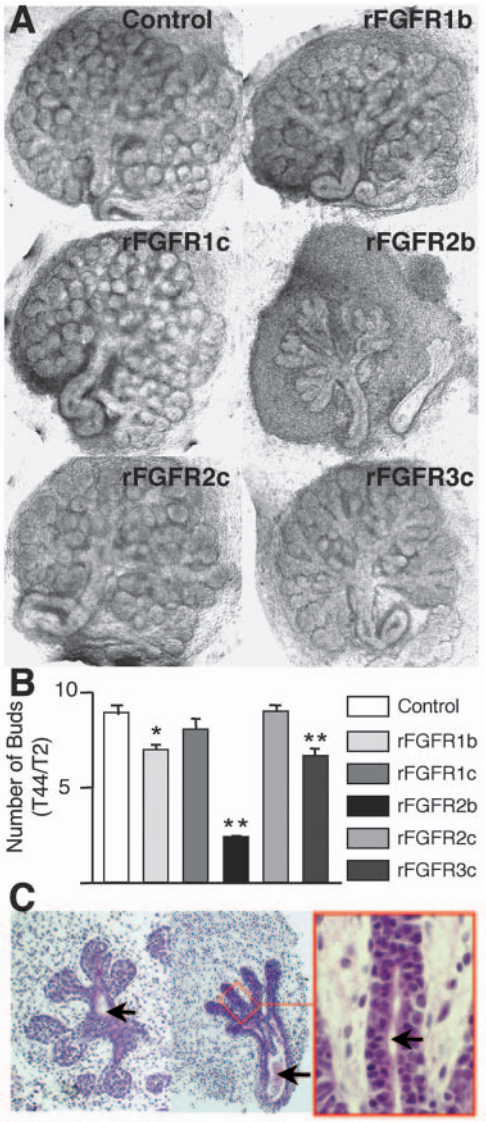

Fig. 2. (A) Soluble recombinant FGFR2b extracellular domain significantly inhibits branching morphogenesis of E13.5 submandibular glands, while rFGFR1b and rFGFR3c have lesser effects (all 10 μg/ml). Taken together, these results suggest that multiple FGFRs are involved in branching morphogenesis. (B) The number of buds was expressed as a ratio of the number of buds at 44 hours/number of buds at 2 hours (T44/T2). At least 5 glands/condition were used for quantitation, and the experiments were repeated at least three times (ANOVA, $*P<0.05$, $**P<0.01$). (C) Hematoxylin and Eosin stained sections show that although rFGFR2b inhibits branching and end bud formation, duct and lumen formation (arrows) still occur. The higher magnification shows duct lumen formation. See Movie 1 in supplementary material of control and rFGFR2b-treated SMGs cultured for 36 hours.

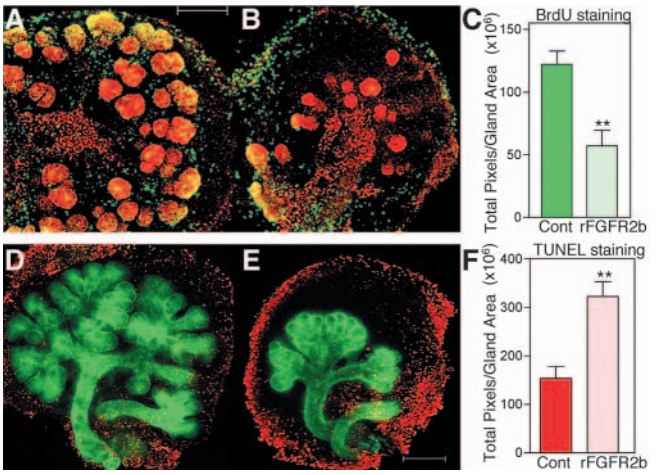

Fig. 3. SMGs treated with rFGFR2b for 44 hours show decreased epithelial cell proliferation (A-C) and increased mesenchyme apoptosis (D-F). Images are maximum projections of optical sections through an entire gland. (A) Control gland shows BrdU labeling (green and yellow) concentrated on the epithelial buds and at the periphery of the mesenchyme. FGFR2 (red) is present mainly on the epithelial buds and on some mesenchyme cells. Scale bar: 200 μm. (B) rFGFR2 treatment results in less BrdU labeling on the epithelial buds. (C) The fluorescent BrdU staining was quantitated (see Materials and methods), and the total fluorescent pixels were expressed as a ratio of the area of the gland. At least five glands/condition were used for quantitation, and the experiments were repeated three times (ANOVA, $**P<0.001$). (D) Apoptosis of mesenchyme cells at the edges and on the surface of the glands in culture was detected with TUNEL staining (red); epithelium was stained with FITC-peanut lectin (green). (E) rFGFR2b treatment increases apoptosis in the mesenchyme, although no epithelial apoptosis is observed. (F) The fluorescent TUNEL staining was quantitated as described above (ANOVA, $**P<0.001$).

treatment dramatically decreased epithelial cell proliferation, but had less effect on mesenchymal cell proliferation. Therefore, the removal of FGFs that bind FGFR2b decreases epithelial proliferation but does not affect FGFR2 localization.

Apoptosis was not detected in the epithelial buds of rFGFR2b-treated glands, but there was a twofold increase in mesenchyme cell apoptosis (Fig. 3D-F), suggesting that the ligands for FGFR2b either directly or indirectly promote survival of the mesenchyme.

FGF7 and FGF10 rescue rFGFR2b-treatment, and neutralizing antibodies to FGF1, FGF7 and FGF10 are required to inhibit branching morphogenesis

Exogenous FGF7 and FGF10 specifically rescued SMGs inhibited with rFGFR2b (Fig. 4A), whereas FGF1, FGF2, FGF3 and BMP7 did not. Soluble rFGFR2b binds to multiple FGFs, therefore we added neutralizing FGF antibodies alone and in combinations to identify the FGFs produced by the endogenous mesenchyme that were required for branching (Fig. 4B). None of the antibodies tested alone could inhibit branching; however, combinations of neutralizing antibodies to FGF1, FGF7 and FGF10 did significantly inhibit branching. These data suggest that multiple FGFs are involved, and that FGF1, FGF7 and FGF10 are important during ex vivo branching morphogenesis.

FGF7 and FGF10 promote distinct epithelial morphogenesis

We used isolated epithelial rudiments cultured in serum-free medium to compare the direct effects of FGFs on epithelial morphogenesis. The epithelial rudiments do not grow without exogenous growth factors and extracellular matrix (ECM).

FGF7 promoted budding of the epithelial rudiment with short ducts in a dose-dependent manner up to 200 ng/ml (Fig. 5A). FGF10 promoted duct elongation without enlargement of the epithelial buds, and increased the length and number of branches in a dose-dependent manner up to 2000 ng/ml (Fig. 5A). FGF1 and FGF4 promoted slight duct elongation, but the epithelium did not continue to grow (Fig. 5A). FGF2 promoted epithelial bud formation in a similar manner to FGF7. Growth factors such as FGF8, FGF18, BMP4 and BMP7 did not support epithelial growth and branching (Fig. 5A).

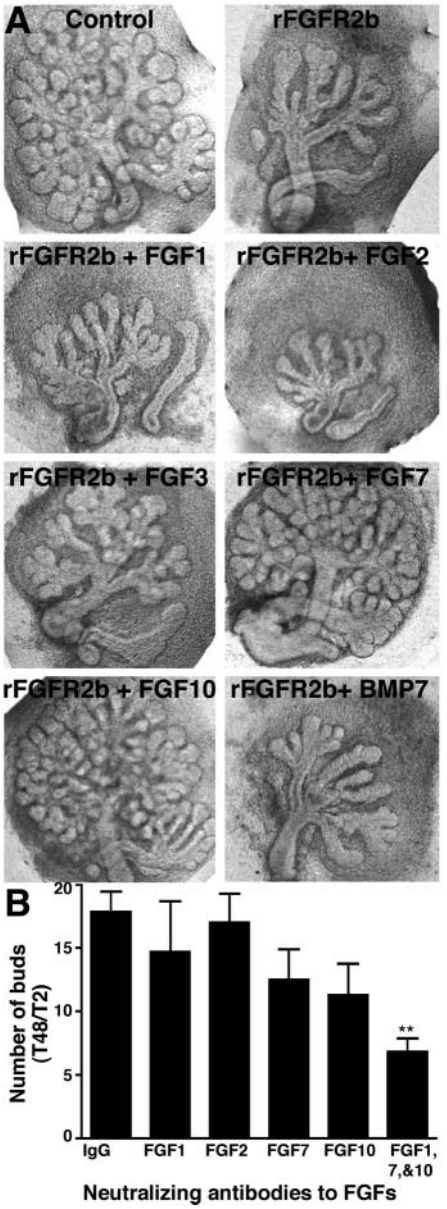

Fig. 4. (A) Glands inhibited with rFGFR2b were rescued with FGF7 and FGF10, which increased the number of end buds. Glands were treated with 1.6 μg/ml of rFGFR2b, and increasing doses of FGFs were added. Glands cultured with rFGFR2b were rescued only by FGF7 (500 ng/ml) and FGF10 (1000 ng/ml), and not by FGF1 (500 ng/ml) and FGF3 (1000 ng/ml), by other ligands for FGFR2b, or by FGF2 (200 ng/ml) or BMP7 (200 ng/ml). (B) A combination of neutralizing antibodies to FGF1, FGF7 and FGF10 was required to significantly inhibit branching morphogenesis (ANOVA, $^{**}P<0.01$). Individual antibodies to FGFs (25 μg/ml), or combinations of either two or three antibodies or similar concentrations of either mouse or goat IgGs, were incubated with E12 SMGs for 48 hours. Individual anti-FGF antibodies or combinations of two anti-FGF antibodies (not shown) did not significantly inhibit branching. The number of buds was expressed as a ratio of the number of buds at 48 hours/number of buds at 2 hours (T48/T2).

We hypothesized that combinations of FGFs binding to both FGFR1b and FGFR2b may result in a more complex morphogenesis. Combinations of FGF2/FGF10, FGF1/FGF7, or FGF1/FGF4 (Fig. 5B) each resulted in phenotypes with more complex morphology than any growth factor alone. FGF1/FGF2/FGF10 resulted in a more complex morphology, similar to in vivo morphogenesis, than any of the dual combinations (Fig. 5B), with elongated ducts, multiple branch points and enlarged epithelial buds. Combinations of FGF10/BMP4 or FGF10/BMP7 did not grow, suggesting that BMPs antagonize FGF10-mediated growth. FGFs and BMPs can play opposing roles in developmental systems involving epithelial-mesenchymal interactions (Neubuser et al., 1997; Niswander and Martin, 1993; Weaver et al., 2000).

FGF-induced morphogenesis is dependent on localized epithelial cell proliferation

Proliferation was measured at 8 hours, prior to morphogenesis, and the ratio of BrdU:SYBR-green was quantitated (Fig. 6A). The FGFs all increased proliferation, BMP4 decreased proliferation, and proliferation in BMP7-treated samples was similar to control (Fig. 6A,B). Therefore, multiple FGFs can stimulate epithelial proliferation, which is independent of later morphogenesis. However, by 44 hours (Fig. 6B) there were distinct patterns of epithelial cell proliferation with different FGFs. Proliferation was concentrated at the tips of the ducts with FGF10 treatment, and occurred throughout the buds and along the ducts with FGF7 treatment. The data suggest that downstream gene expression may regulate factors that specify where localized proliferation occurs. Either the localization of the FGFRs or the expression of downstream mediators of morphogenesis could specify the sites of proliferation.

FGFR1 and FGFR2 are present throughout the epithelium

Whole-mount immunolocalization of FGFR1 and FGFR2 in both FGF7- and FGF10-treated epithelial rudiments reveals that both receptors are expressed throughout the epithelium (Fig. 7A,B). Staining with both antibodies was blocked by pre-incubation with the immunizing peptides to which the antibodies were raised. There was increased FGFR1 staining around the periphery of the buds with FGF7 treatment and at the tips of the buds with FGF10 treatment. E-cadherin staining highlights the cell-cell junctions and acts as a control for antibody penetration through the tissue, while SYBR-green stains the nucleus of the cells and is pseudo-colored blue (Fig. 7A,B). Thus, FGFR localization alone does not specify where FGF7- or FGF10-induced proliferation occurs; therefore, possible co-receptors or cofactors may be involved, and multiple signaling pathways may exist if co-receptors are present.

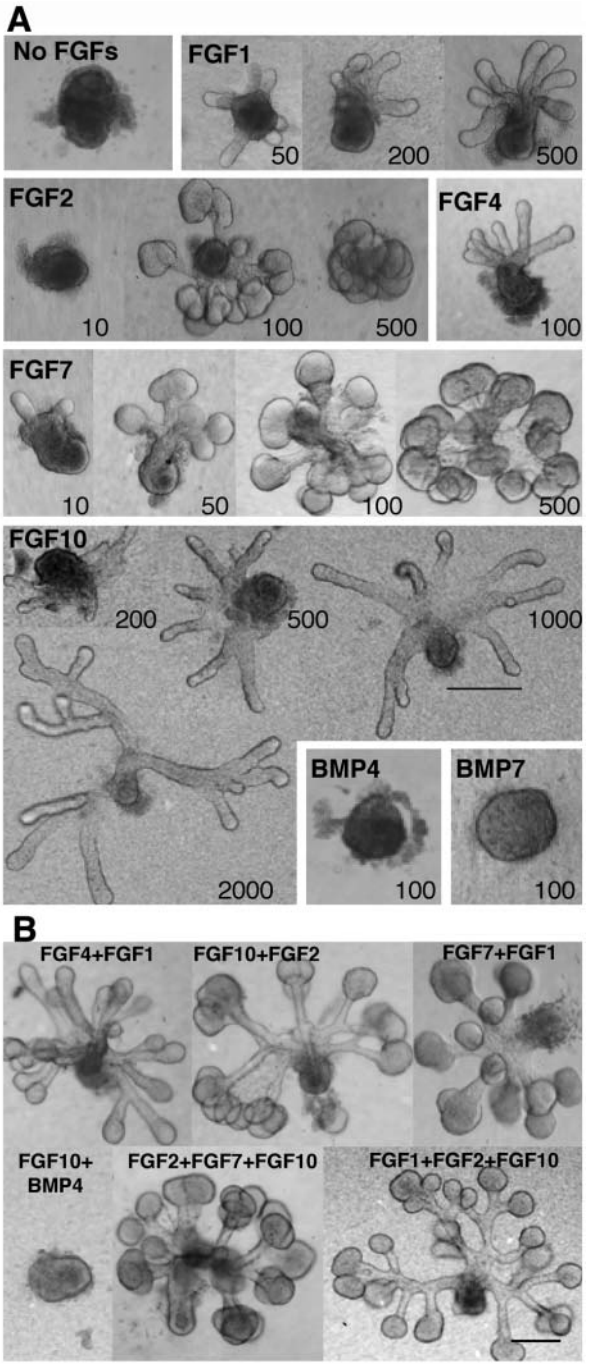

Fig. 5. (A) Individual FGFs and BMPs have distinct morphological effects on isolated epithelium cultured in growth factor-reduced Matrigel for 44 hours. FGF1-, FGF4- and FGF10-treated epithelium form duct-like structures, whereas FGF2 and FGF7 promote bud formation. Epithelium treated with FGF8, BMP4 or BMP7 alone do not grow. Numbers indicate concentrations in ng/ml. (B) Combinations of FGFs resulted in phenotypes with more complex morphology than any growth factor alone. FGF4/FGF1 resulted in larger glands with longer ducts. FGF10/FGF2 and FGF7/FGF1 both resulted in elongated stalks and enlarged buds. Combinations of FGF10 or FGF7 with either BMP4 (shown) or BMP7 (similar result, not shown) did not grow, suggesting BMPs antagonize FGF7 and FGF10. FGF2/FGF7/FGF10 resulted in multiple stalks and buds. FGF1/FGF2/FGF10 resulted in the most complex morphology with elongated ducts, multiple branch points and enlarged terminal epithelial buds. Scale bars: 200 μm.

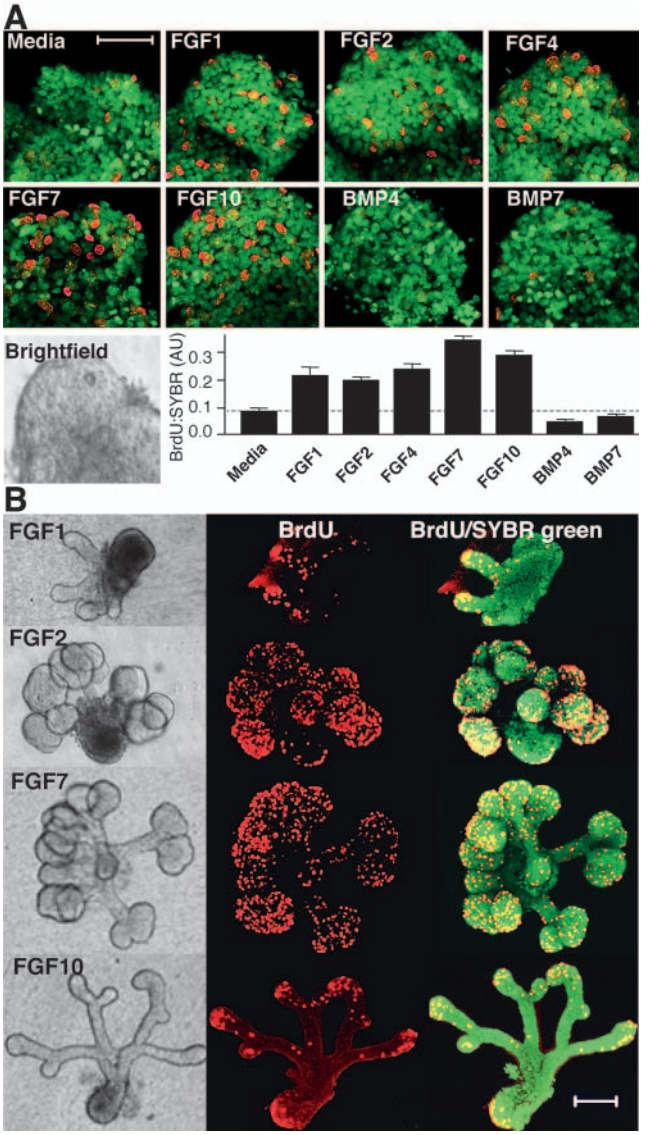

Fig. 6. FGF-induced morphogenesis is a result of localized proliferation. (A) Individual FGFs, FGF1 (200 ng/ml), FGF2 (100 ng/ml), FGF4 (100 ng/ml), FGF7 (100 ng/ml) and FGF10 (500 ng/ml), stimulate proliferation of epithelial buds by 8 hours, before any morphogenesis has occurred. BMP4 (100 ng/ml) and BMP7 (100 ng/ml) did not stimulate epithelial proliferation above control levels. Scale bar: 50 μm. BrdU was detected with a Cy3-labeled antibody, the nuclei were stained with SYBR-green, and fluorescence was quantitated using MetaMorph software and expressed as the ratio of BrdU:SYBR-green pixels. At least five glands/condition were used for quantitation, and the experiments were repeated twice with similar results. (B) FGFs induce localized proliferation resulting in distinct morphologies by 44 hours. FGF1 and FGF10 stimulate proliferation at the tips of the ducts. FGF2 and FGF7 stimulate proliferation over the entire buds, and FGF7 also induces duct proliferation. BrdU was detected with a Cy3-labeled antibody, and nuclei were stained with SYBR-green. Scale bar: 100 μm.

Downstream signaling from FGF7 and FGF10 is Mek1/2 dependent; FGF7 signaling is also PI3K-dependent

Chemical inhibitors and recombinant FGFRs were added to epithelial rudiments to identify the receptors and downstream pathways of FGF7 and FGF10 (Fig. 8). Su5402 (2.5 μM), an inhibitor of FGFR phosphorylation, UO126 (10 μM), a MEK1/2 inhibitor, and rFGFR2b (1.6 μg/ml) all significantly inhibited FGF7- and FGF10-mediated morphogenesis. They all resulted in a decrease in bud number with FGF7 treatment and a reduction in the length of the ducts with FGF10 treatment (Fig. 8B). However, LY294002 (10 μM), a PI3K inhibitor, inhibited FGF7-mediated morphogenesis but not FGF10-mediated morphogenesis, and GO6983 (1.5 μM), a broad PKC inhibitor, did not inhibit morphogenesis (Fig. 8A,B). In addition, rFGFR1b did not inhibit growth, but it did alter the morphology of FGF7-treated epithelium, resulting in a slight, but not significant, increase in bud number with more prominent ducts. This may suggest that FGFR1b plays a role in FGF7-mediated morphogenesis, possibly downstream of FGF7/FGFR2b signaling. Taken together, these data suggest that epithelial budding requires both PI3K- and MEK1/2-dependent signaling, whereas duct elongation requires MEK1/2-dependent signaling. Therefore, downstream gene expression from FGF7 and FGF10 signaling must result in differential expression of the mediators of morphogenesis.

FGF7 increases FGFR1b and FGF1 expression, and FGF-mediated morphogenesis is MMP-dependent

The downstream mediators of morphogenesis likely involve the interplay between MMPs and growth factors (Simian et al., 2001). We compared levels of *MMP*, *FGF* and *FGFR* gene expression after FGF7 or FGF10 treatment by real-time PCR. Expression was normalized to *S29* and expressed as a fold change in expression with FGF7 treatment compared with FGF10 treatment (Fig. 9B). Exogenous FGF7 increased expression of *MMP2* (3.4-fold), *FGF1* (4.1-fold) and *FGFR1b* (1.8-fold) compared with the levels of expression with FGF10 treatment. FGF10 treatment increased expression of *MMP9* (2.9-fold) and *FGFR2b* (1.5-fold) compared with FGF7 treatment, although *MMP9* expression was much lower (~500-fold less) than *MMP2* expression based on the threshold values of the PCR reactions. *MMP14* (also known as *MT1-MMP*) was expressed at similar levels with either FGF7 or FGF10 treatment.

The pattern of immunolocalization of MMP2 and MMP9 was similar in whole SMGs and epithelial rudiments. MMP2 was localized in the mesenchyme and the peripheral epithelial cells in the whole gland (Fig. 9A, part a), whereas MMP9 was only localized in the mesenchyme (Fig. 9A, part b). Perlecan staining in the mesenchyme and the basement membrane outlines the epithelium in confocal sections. In FGF7- or FGF10-treated epithelium, MMP2 was localized in the cells near the periphery of the rudiment (Fig. 9A, part c,d). MMP9 was localized in the few mesenchyme cells remaining after the mechanical separation of epithelium and mesenchyme, and was not present in the epithelium (Fig. 9A, part e,f). The MMP9 mesenchyme staining explains why MMP9 was much less abundant than MMP2 in the real-time PCR. The cells positive for MMP9 did not stain with α6 integrin (Fig. 9A, part e), an epithelial marker, but did stain with perlecan, a mesenchyme marker (data not shown).

We analyzed MMP activity in the conditioned media by gelatin zymography, after 24 and 44 hours of FGF treatment (Fig. 9C). FGF7 increased both the pro and active forms of MMP2 when compared with FGF10. FGF10 increased MMP9 levels when compared with FGF7, although MMP9 is barely detectable by zymograms, as a few remaining mesenchyme cells produced it. Therefore, the changes in *MMP* gene expression are consistent with the changes in MMP activity. Epithelial morphogenesis is dependent on MMP activity, since GM6001, a broad MMP inhibitor, inhibited the enlargement of the epithelial buds and elongation of the ducts (Fig. 9D). In addition, neutralizing antibodies to FGF1 were required to inhibit morphogenesis in the intact SMG, so we added them to FGF7- and FGF10-treated epithelium. Anti-FGF1 inhibited growth, suggesting the epithelial production of FGF1 was

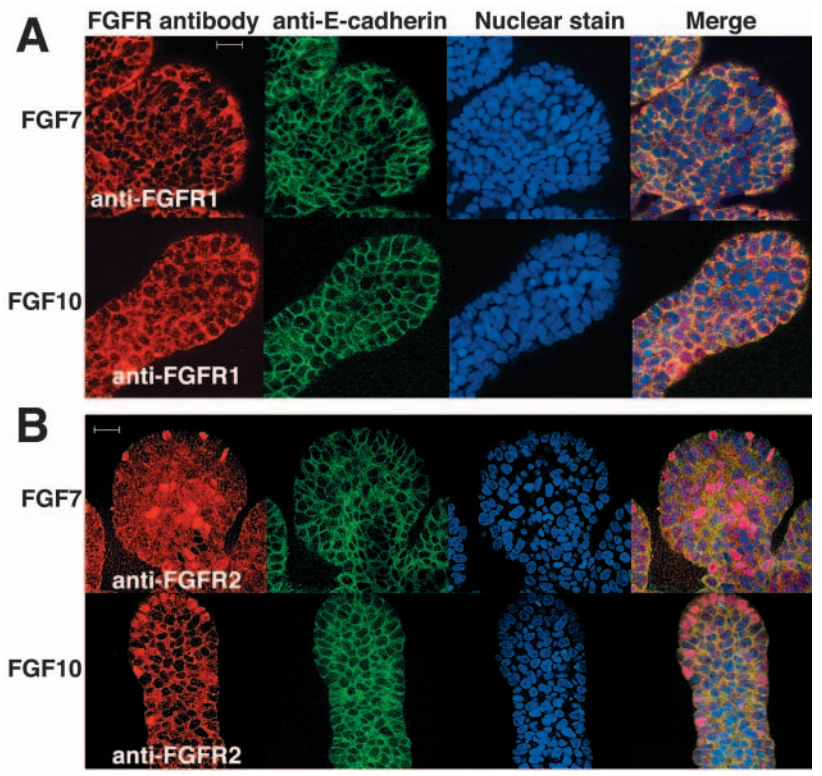

Fig. 7. FGFR1 and FGFR2 are expressed throughout the epithelium. (A) FGFR1 staining (red) is increased around the edge of the bud with FGF7 treatment, and near the tip of the duct with FGF10 treatment. E-cadherin (green) defines the cell junctions of the epithelium, and SYBR-green stains the nucleus (pseudocolored blue). (B) FGFR2 staining (red) is localized throughout the epithelium in a punctate pattern and shows less cell membrane localization with FGF7 than with FGF10 treatment. E-cadherin (green) defines the cell junctions of the epithelium and SYBR-green stains the nucleus (pseudocolored blue). Scale bars: 20 μm.

required for FGF7- and FGF10-mediated morphogenesis. These data also support the hypothesis that FGF1 signaling (which may be through FGFR1b) and FGFR2b are required for branching morphogenesis. Taken together, our data suggest that MMP and FGF1 are mediators of morphogenesis, and are required for both FGF7- and FGF10-dependent morphogenesis.

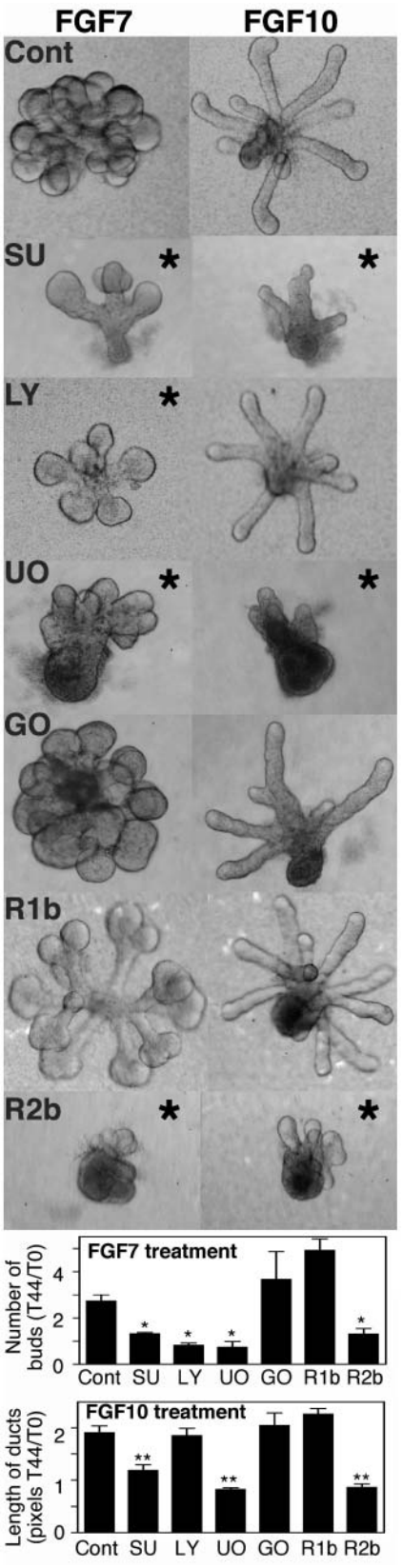

Discussion

FGFR2b is important for the initiation of salivary gland development, as mice lacking *FGFR2b* do not develop glands (De Moerlooze et al., 2000). The mechanisms of FGFR2b and FGF action during branching morphogenesis, after gland initiation occurs, are unknown. Here, we report that FGF7- and FGF10-mediated FGFR2b signaling regulates submandibular gland epithelial morphogenesis ex vivo by inducing localized proliferation and increased expression of *FGFR1b*/*FGF1* and MMP2, and that both FGF1 and MMP activity are required for FGF-mediated epithelial morphogenesis.

Multiple FGFs and FGFRs are present in SMGs (Hoffman et al., 2002), and defining which FGFs are important in SMG development is hampered by the fact that many FGFs have overlapping functions. FGF10-knockout mice have no salivary glands (Ohuchi et al., 2000), suggesting that gland initiation is dependent on FGF10, but our ex vivo data suggest that, once the gland has formed, inhibition of FGF10 with neutralizing antibodies or decreasing *FGF10* expression by antisense treatment (M.P.H., unpublished) does not inhibit branching. The lack of a SMG phenotype in single FGF-null mice, such as the FGF2- and FGF7-null mice (Sun et al., 2002; Zhou et al., 1998), could be interpreted as meaning they are not important for SMG development; however, overlapping FGF function is likely to compensate during development. Our experiments requiring combinations of neutralizing FGF1, FGF7 and FGF10 antibodies to inhibit branching when the endogenous mesenchyme is present support this hypothesis.

Previous reports show that FGF7 induces SMG epithelial proliferation but that epithelial budding also requires EGFR ligation (Morita and Nogawa, 1999). However, media with 10% horse serum was used in these experiments, which contains mitogenic growth factors and makes comparison difficult with our serum-free conditions. The EGFR-null mouse (Jaskoll and Melnick, 1999) has macroscopically normal glands with a reduction of buds/area, suggesting that EGFR regulates SMG branch number in vivo but is not essential for SMG initiation or early branching. An exogenous EGFR ligand is not required for epithelial branching; however, the ECM may contain EGFR ligands or the epithelium may produce an endogenous EGFR ligand. MMP degradation of

Fig. 8. FGF7- and FGF10-mediated morphogenesis is ERK1/2 dependent. FGF7-mediated morphogenesis is also PI3K dependent. FGF7- (200 ng/ml) and FGF10- (1500 ng/ml) mediated morphogenesis is inhibited by the FGFR inhibitor SU5402 (SU, 2.5 μM), the MEK1/2 inhibitor UO126 (UO, 10 μM), and by rFGFR2b (R2b, 5 μg/ml), but not by the broad PKC inhibitor GO6983 (GO, 1.5 μM), or by rFGFR1b (R1b, 10 μg/ml). FGF7-mediated morphogenesis is also inhibited by the PI3K inhibitor LY294002 (LY, 10 μM). Star indicates an inhibited phenotype. The inhibitors were added to the media for 44 hours, and the number of buds (for FGF7) and the length of ducts (for FGF10) were measured using MetaMorph software and expressed as a ratio at 44 hours/time 0. *, $P<0.5$; **, $P<0.01$. See Movie 2 in supplementary material, which shows FGF7- and FGF10-treated epithelium cultured for 36 hours.

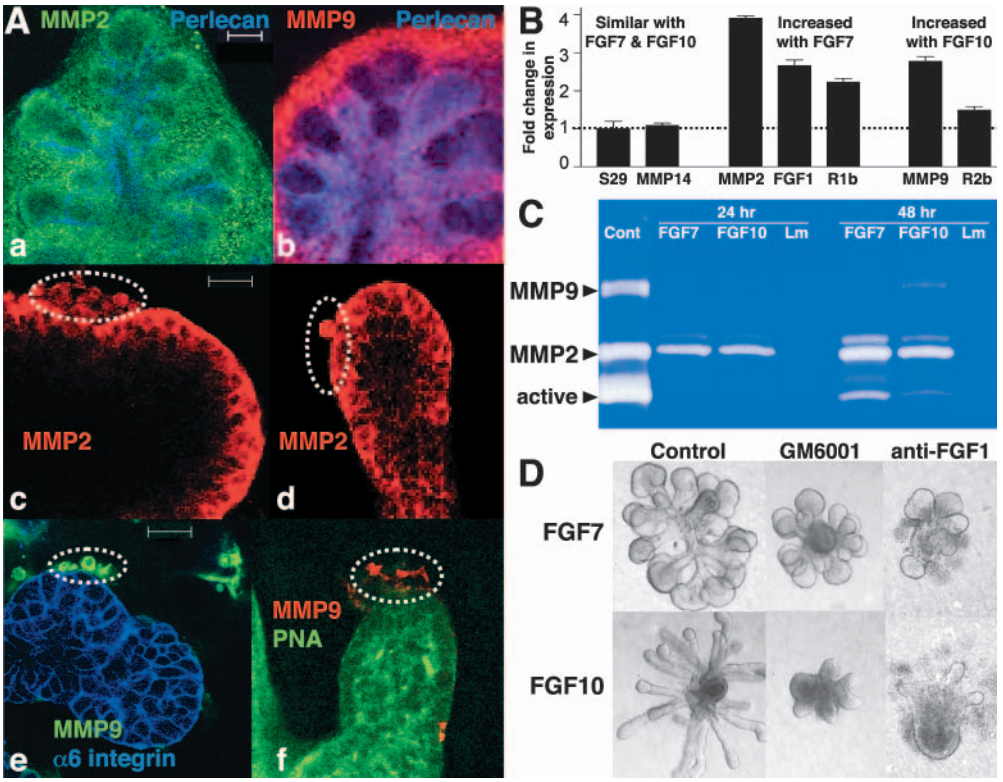

Fig. 9. FGF-mediated morphogenesis is MMP-dependent. (A, part a,b) MMP2 is localized in the mesenchyme and in the epithelium at the periphery of the growing buds, while MMP9 is localized only in the mesenchyme. Perlecan, produced by the mesenchyme, stains the basement membrane. LSCM sections of E13 cultured glands. Scale bar: 100 μm. (A, part c,d) MMP2 is localized at the periphery of the epithelium and in residual mesenchyme cells (dotted outline) in both (c) FGF7- and (d) FGF10-treated epithelium. (A, part e,f) MMP9 is localized only in the residual mesenchyme cells (dotted outline) in both FGF7- and FGF10-treated epithelium. α6 integrin and peanut lectin (PNA) are epithelial cell markers. Scale bars: 20 μm. (B) The relative levels of gene expression of *MMPs*, *FGFs* and *FGFRs* were compared by real-time PCR in salivary epithelium treated with either FGF7 (200 ng/ml) or FGF10 (1500 ng/ml) for 44 hours. *MMP2* gene expression was increased ~4-fold, *FGF1* expression was increased ~2.5-fold and *FGFR1b* expression was increased ~2-fold in FGF7-treated epithelial rudiments, when compared with FGF10-treated epithelial rudiments. (C) FGF7 increases MMP2 production and activation after 44 hours. The culture media from epithelium treated with FGF7 or FGF10, as well as media from a dish with laminin-1 alone, was assayed by gelatin zymography after 24 and 44 hours of FGF treatment. (D) FGF7- and FGF10-mediated morphogenesis is inhibited by GM6001 (5 μM), a broad MMP inhibitor, and by a neutralizing antibody to FGF1 (25 μg/ml). Neither a DMSO carrier control (shown) nor an IgG control (not shown) inhibited morphogenesis.

laminin-5 is reported to release an EGF-like fragment during mammary involution (Schenk et al., 2003).

We have identified striking morphological differences between FGF7- and FGF10-treated SMG epithelium (Fig. 5). The function of FGFs in SMG epithelium is different from other branching organs. In the lung, FGF10 plays an important role during morphogenesis and induces primary and secondary bud formation, FGF1 induces robust growth with elongated buds, and FGF7 induces a cyst-like structure (Bellusci et al., 1997; Cardoso et al., 1997; Izvolsky et al., 2003a; Weaver et al., 2000). During uteric bud outgrowth, FGF1 and FGF7 are at opposite ends of a morphogenic spectrum, with FGF10 and FGF2 in between (Qiao et al., 2001). FGF1 induces elongated uteric buds with proliferating tips, whereas FGF7 induces proliferation with an amorphous morphology.

FGF10 is involved in Harderian and lacrimal gland development, where it induces epithelial proliferation but not branching morphogenesis (Govindarajan et al., 2000; Makarenkova et al., 2000). FGF10 is important during tooth development (Kettunen et al., 2000), where it is a survival factor for stem cell populations (Harada et al., 2002). In SMG epithelium, FGF10 promotes duct elongation by localized proliferation at the tip of the duct through ERK1/2-dependent pathways. Nuclear localization of FGFRs has been reported (Wells and Marti, 2002), and FGFR2 was recently found in the nucleus during FGF9-induced proliferation (Schmahl et al., 2004). FGFR1b and FGFR2b are also localized throughout the epithelium; therefore, a co-receptor or cofactor is likely to be required to allow FGF10 to specifically stimulate just the tip cells to proliferate. The most likely candidates are heparan sulfate-containing cofactors or receptors, on the cell surface or in the ECM. The mitogenic activity of FGF10 is stimulated by heparin, whereas FGF7 is inhibited (Igarashi et al., 1998), suggesting the effects of FGF7 and FGF10 may be regulated by heparan sulfate. In the lung bud, the localization of heparan sulfate isoforms regulates FGF function at a particular stage or localization during development (Izvolsky et al., 2003a; Izvolsky et al., 2003b), although other transmembrane regulators of FGF signaling such as *sef* and *XFLRT3* could be involved (Tsang and Dawid, 2004). This hypothesis remains to be tested in the context of salivary gland morphogenesis.

Both FGF7 and FGF10 signal through FGFR2b in

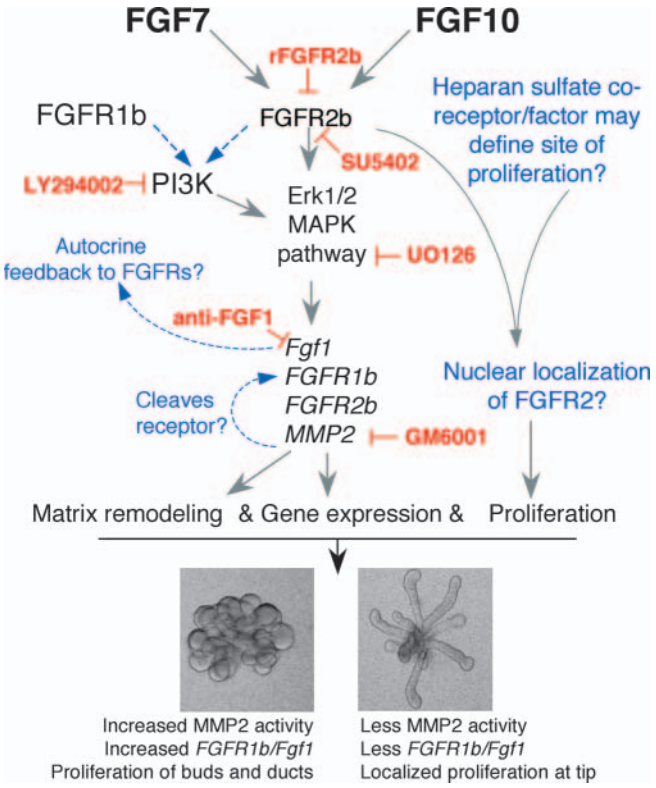

Fig. 10. Working model of how FGF7 and FGF10 signaling through FGFR2b regulates morphogenesis. The model summarizes our findings, and the dotted lines show other potential mechanisms: MMP2 may regulate FGFR1 cleavage; FGF1 expression may stimulate both FGFR1 and FGFR2; cofactors or co-receptors may specify the localization of FGF binding and, therefore, where proliferation occurs.

an ERK1/2-dependent manner, but FGF7-mediated morphogenesis is also PI3K-dependant. In corneal epithelial cells, FGF7 also stimulates PI3K activity but is not inhibited by MAPK inhibitors (Chandrasekher et al., 2001). In our studies, FGF7 also increased *FGFR1b* and *FGF1* expression compared with FGF10. The PI3K-dependent pathway (Fig. 8) and FGF1 activity (Fig. 9D) are both necessary for epithelial budding. PI3K may be downstream from either FGF10/FGFR1b, or from FGF1 binding either FGFR1b or FGFR2b. Therefore the downstream signaling from FGF7 may act in concert with FGF1 signaling to increase widespread proliferation resulting in epithelial budding. FGF-mediated increases in FGF gene expression have been identified in other systems, such as the lung, where FGF7 also increases expression of *FGF1* (Lebeche et al., 1999). Many studies on FGFR signaling focus on the roles of FGF1 and FGF2 in either migration or proliferation, and suggest that cells use Src and p38MAPK for migration and ERKs for proliferation (Boilly et al., 2000). Our data show that ERKs are necessary for proliferation; however, the role of cell migration is clearly important in SMG morphogenesis (see Movies 1 and 2 in supplementary material), and identifying the mechanisms of cell migration will be important for understanding gland development.

There is increasing evidence that MMPs, in concert with FGFs, regulate morphogenesis (Simian et al., 2001). In breast cancer and lung epithelium, FGFs increase MMP production (Liu et al., 2002; Miura and Shiota, 2002). MMP2 cleaves the extracellular FGFR1, releasing a fragment that binds FGFs (Levi et al., 1996). Our data show that FGF7 increases MMP2 expression and activation, and *FGFR1b* expression, which may allow the expanding epithelium to remodel the ECM and release soluble FGFR1b to regulate FGF function in a similar manner to our rFGFR experiments (Figs 2, 8). Expression profiling of MMPs in the salivary epithelium and mesenchyme reveal that most MMPs are expressed in the mesenchyme, except MMP2 and the two membrane-bound MMPs, MMP14 and MMP15 (M.P.H., unpublished). The epithelial localization of MMP2 around the periphery of the expanding bud and elongating duct, the inhibition of morphogenesis with an MMP inhibitor, and the lack of MMP9 in the epithelium suggest that MMP2 activation is important for epithelial morphogenesis. Information about the function of MMPs from individual knockouts has not revealed much about their role in development. MMP2-null mice are viable, although smaller, and are fertile (Itoh et al., 1997), whereas the MMP14 mouse has skeletal defects due to a lack of collagen turnover (Holmbeck et al., 1999). However, recently the MMP2/MMP14 double-knockout mouse was reported (Oh et al., 2004); the mice die after birth with respiratory failure, abnormal blood vessels and immature muscle fibers, suggesting a major developmental phenotype. Neither the phenotype of the salivary glands nor detailed analysis of organogenesis was reported, but the increased severity of the phenotype suggests that MMP2 and MMP14 play important roles during development that are not revealed by the single knockout. This report highlights the difficulties of drawing conclusions about in vivo function from the analysis of single gene knockouts in large families of proteins with overlapping functions, such as the FGFs and MMPs.

In conclusion, branching morphogenesis of mouse submandibular glands ex vivo is regulated by multiple FGFs and FGFRs. Downstream of FGF7 or FGF10 binding to FGFR2b there is a regulatory network of *FGFR1b*/*FGF1*/*MMP2* expression that influences morphogenesis. Localized cell proliferation results in either epithelial budding or duct elongation. Increased MMP2 activity may increase ECM remodeling and FGFR cleavage, allowing localized expansion of the epithelium into the ECM at sites where proliferation occurs. The increased expression of *FGFR1* and *FGF1* with FGF7 could reinforce epithelial proliferation in an autocrine manner, resulting in widespread proliferation and budding. On the contrary, FGF10 treatment results in elongation of the duct behind the proliferating tip, where co-receptors or cofactors define the site of FGF10/FGFR2b signaling. The difference between FGF7-and FGF10-mediated morphogenesis is likely to be due to the factors that localize FGF binding to specific cells expressing FGFRs, resulting in different amounts of FGFR2b signaling, proliferation, and downstream expression of autocrine FGF signaling loops and proteases. Therefore, identifying the co-receptors or cofactors that regulate localized FGF binding and FGFR activation in the developing submandibular gland is an important future goal.

The authors thank Harry Grant and Rouman Pankov for critical reading of the manuscript, and Hynda Kleinman for her outstanding mentoring and support.

Supplementary material

Supplementary material for this article is available at
http://dev.biologists.org/cgi/content/full/132/6/1223/DC1

References

Bellusci, S., Grindley, J., Emoto, H., Itoh, N. and Hogan, B. L. (1997). Fibroblast growth factor 10 (FGF10) and branching morphogenesis in the embryonic mouse lung. *Development* **124**, 4867-4878.

Boilly, B., Vercoutter-Edouart, A. S., Hondermarck, H., Nurcombe, V. and Le Bourhis, X. (2000). FGF signals for cell proliferation and migration through different pathways. *Cytokine Growth Factor Rev.* **11**, 295-302.

Cardoso, W. V., Itoh, A., Nogawa, H., Mason, I. and Brody, J. S. (1997). FGF-1 and FGF-7 induce distinct patterns of growth and differentiation in embryonic lung epithelium. *Dev. Dyn.* **208**, 398-405.

Celli, G., LaRochelle, W. J., Mackem, S., Sharp, R. and Merlino, G. (1998). Soluble dominant-negative receptor uncovers essential roles for fibroblast growth factors in multi-organ induction and patterning. *EMBO J.* **17**, 1642-1655.

Chandrasekher, G., Kakazu, A. H. and Bazan, H. E. (2001). HGF- and KGF-induced activation of PI-3K/p70 s6 kinase pathway in corneal epithelial cells: its relevance in wound healing. *Exp. Eye Res.* **73**, 191-202.

De Moerlooze, L., Spencer-Dene, B., Revest, J., Hajihosseini, M., Rosewell, I. and Dickson, C. (2000). An important role for the IIIb isoform of fibroblast growth factor receptor 2 (FGFR2) in mesenchymal-epithelial signalling during mouse organogenesis. *Development* **127**, 483-492.

Govindarajan, V., Ito, M., Makarenkova, H. P., Lang, R. A. and Overbeek, P. A. (2000). Endogenous and ectopic gland induction by FGF-10. *Dev. Biol.* **225**, 188-200.

Guo, L., Yu, Q. C. and Fuchs, E. (1993). Targeting expression of keratinocyte growth factor to keratinocytes elicits striking changes in epithelial differentiation in transgenic mice. *EMBO J.* **12**, 973-986.

Guo, L., Degenstein, L. and Fuchs, E. (1996). Keratinocyte growth factor is required for hair development but not for wound healing. *Genes Dev.* **10**, 165-175.

Harada, H., Toyono, T., Toyoshima, K., Yamasaki, M., Itoh, N., Kato, S., Sekine, K. and Ohuchi, H. (2002). FGF10 maintains stem cell compartment in developing mouse incisors. *Development* **129**, 1533-1541.

Hayakawa, T., Kishi, J. and Nakanishi, Y. (1992). Salivary gland morphogenesis: possible involvement of collagenase. *Matrix Suppl.* **1**, 344-351.

Hoffman, M. P., Kidder, B. L., Steinberg, Z. L., Lakhani, S., Ho, S., Kleinman, H. K. and Larsen, M. (2002). Gene expression profiles of mouse submandibular gland development: FGFR1 regulates branching morphogenesis in vitro through BMP- and FGF-dependent mechanisms. *Development* **129**, 5767-5778.

Holmbeck, K., Bianco, P., Caterina, J., Yamada, S., Kromer, M., Kuznetsov, S. A., Mankani, M., Robey, P. G., Poole, A. R., Pidoux, I. et al. (1999). MT1-MMP-deficient mice develop dwarfism, osteopenia, arthritis, and connective tissue disease due to inadequate collagen turnover. *Cell* **99**, 81-92.

Igarashi, M., Finch, P. W. and Aaronson, S. A. (1998). Characterization of recombinant human fibroblast growth factor (FGF)-10 reveals functional similarities with keratinocyte growth factor (FGF-7). *J. Biol. Chem.* **273**, 13230-13235.

Itoh, T., Ikeda, T., Gomi, H., Nakao, S., Suzuki, T. and Itohara, S. (1997). Unaltered secretion of beta-amyloid precursor protein in gelatinase A (matrix metalloproteinase 2)-deficient mice. *J. Biol. Chem.* **272**, 22389-22392.

Izvolsky, K. I., Shoykhet, D., Yang, Y., Yu, Q., Nugent, M. A. and Cardoso, W. V. (2003a). Heparan sulfate-FGF10 interactions during lung morphogenesis. *Dev. Biol.* **258**, 185-200.

Izvolsky, K. I., Zhong, L., Wei, L., Yu, Q., Nugent, M. A. and Cardoso, W. V. (2003b). Heparan sulfates expressed in the distal lung are required for Fgf10 binding to the epithelium and for airway branching. *Am. J. Physiol. Lung Cell Mol. Physiol.* **285**, L838-L846.

Jaskoll, T. and Melnick, M. (1999). Submandibular gland morphogenesis: stage-specific expression of TGF-alpha/EGF, IGF, TGF-beta, TNF, and IL-6 signal transduction in normal embryonic mice and the phenotypic effects of TGF-beta2, TGF-beta3, and EGF-r null mutations. *Anat. Rec.* **256**, 252-268.

Jaskoll, T., Zhou, Y. M., Chai, Y., Makarenkova, H. P., Collinson, J. M., West, J. D., Hajihosseini, M. K., Lee, J. and Melnick, M. (2002). Embryonic submandibular gland morphogenesis: stage-specific protein localization of FGFs, BMPs, Pax6 and Pax9 in normal mice and abnormal SMG phenotypes in FgfR2-IIIc(+/Delta), BMP7(–/–) and Pax6(–/–) mice. *Cells Tissues Organs* **170**, 83-98.

Jaskoll, T., Witcher, D., Toreno, L., Bringas, P., Moon, A. M. and Melnick, M. (2004). FGF8 dose-dependent regulation of embryonic submandibular salivary gland morphogenesis. *Dev. Biol.* **268**, 457-469.

Kashimata, M. and Gresik, E. W. (1997). Epidermal growth factor system is a physiological regulator of development of the mouse fetal submandibular gland and regulates expression of the alpha6-integrin subunit. *Dev. Dyn.* **208**, 149-161.

Kashimata, M., Sayeed, S., Ka, A., Onetti-Muda, A., Sakagami, H., Faraggiana, T. and Gresik, E. W. (2000). The ERK-1/2 signaling pathway is involved in the stimulation of branching morphogenesis of fetal mouse submandibular glands by EGF. *Dev. Biol.* **220**, 183-196.

Kettunen, P., Laurikkala, J., Itaranta, P., Vainio, S., Itoh, N. and Thesleff, I. (2000). Associations of FGF-3 and FGF-10 with signaling networks regulating tooth morphogenesis. *Dev. Dyn.* **219**, 322-332.

Larsen, M., Hoffman, M. P., Sakai, T., Neibaur, J. C., Mitchell, J. M. and Yamada, K. M. (2003). Role of PI 3-kinase and PIP3 in submandibular gland branching morphogenesis. *Dev. Biol.* **255**, 178-191.

Lebeche, D., Malpel, S. and Cardoso, W. V. (1999). Fibroblast growth factor interactions in the developing lung. *Mech. Dev.* **86**, 125-136.

Levi, E., Fridman, R., Miao, H. Q., Ma, Y. S., Yayon, A. and Vlodavsky, I. (1996). Matrix metalloproteinase 2 releases active soluble ectodomain of fibroblast growth factor receptor 1. *Proc. Natl. Acad. Sci. USA* **93**, 7069-7074.

Liu, J. F., Crepin, M., Liu, J. M., Barritault, D. and Ledoux, D. (2002). FGF-2 and TPA induce matrix metalloproteinase-9 secretion in MCF-7 cells through PKC activation of the Ras/ERK pathway. *Biochem. Biophys. Res. Commun.* **293**, 1174-1182.

Makarenkova, H. P., Ito, M., Govindarajan, V., Faber, S. C., Sun, L., McMahon, G., Overbeek, P. A. and Lang, R. A. (2000). FGF10 is an inducer and Pax6 a competence factor for lacrimal gland development. *Development* **127**, 2563-2572.

Martin, G. R. (1998). The roles of FGFs in the early development of vertebrate limbs. *Genes Dev.* **12**, 1571-1586.

Min, H., Danilenko, D. M., Scully, S. A., Bolon, B., Ring, B. D., Tarpley, J. E., DeRose, M. and Simonet, W. S. (1998). Fgf-10 is required for both limb and lung development and exhibits striking functional similarity to Drosophila branchless. *Genes Dev.* **12**, 3156-3161.

Miura, T. and Shiota, K. (2002). Depletion of FGF acts as a lateral inhibitory factor in lung branching morphogenesis in vitro. *Mech. Dev.* **116**, 29-38.

Morita, K. and Nogawa, H. (1999). EGF-dependent lobule formation and FGF7-dependent stalk elongation in branching morphogenesis of mouse salivary epithelium in vitro. *Dev. Dyn.* **215**, 148-154.

Nakanishi, Y., Sugiura, F., Kishi, J. and Hayakawa, T. (1986). Collagenase inhibitor stimulates cleft formation during early morphogenesis of mouse salivary gland. *Dev. Biol.* **113**, 201-206.

Neubuser, A., Peters, H., Balling, R. and Martin, G. R. (1997). Antagonistic interactions between FGF and BMP signaling pathways: a mechanism for positioning the sites of tooth formation. *Cell* **90**, 247-255.

Niswander, L. and Martin, G. R. (1993). FGF-4 and BMP-2 have opposite effects on limb growth. *Nature* **361**, 68-71.

Oh, J., Takahashi, R., Adachi, E., Kondo, S., Kuratomi, S., Noma, A., Alexander, D. B., Motoda, H., Okada, A., Seiki, M. et al. (2004). Mutations in two matrix metalloproteinase genes, MMP-2 and MT1-MMP, are synthetic lethal in mice. *Oncogene* **23**, 5041-5048.

Ohuchi, H., Hori, Y., Yamasaki, M., Harada, H., Sekine, K., Kato, S. and Itoh, N. (2000). FGF10 acts as a major ligand for FGF receptor 2 IIIb in mouse multi-organ development. *Biochem. Biophys. Res. Commun.* **277**, 643-649.

Ornitz, D. M. (2000). FGFs, heparan sulfate and FGFRs: complex interactions essential for development. *BioEssays* **22**, 108-112.

Ornitz, D. M. and Itoh, N. (2001). Fibroblast growth factors. *Genome Biol.* **2**, REVIEWS3005.

Pohl, M., Sakurai, H., Bush, K. T. and Nigam, S. K. (2000). Matrix metalloproteinases and their inhibitors regulate in vitro ureteric bud branching morphogenesis. *Am. J. Physiol. Renal Physiol.* **279**, F891-F900.

Post, M., Souza, P., Liu, J., Tseu, I., Wang, J., Kuliszewski, M. and Tanswell, A. K. (1996). Keratinocyte growth factor and its receptor are involved in regulating early lung branching. *Development* **122**, 3107-3115.

Powers, C. J., McLeskey, S. W. and Wellstein, A. (2000). Fibroblast growth factors, their receptors and signaling. *Endocr. Relat. Cancer* **7**, 165-197.

Qiao, J., Uzzo, R., Obara-Ishihara, T., Degenstein, L., Fuchs, E. and Herzlinger, D. (1999). FGF-7 modulates ureteric bud growth and nephron number in the developing kidney. *Development* **126**, 547-554.

Qiao, J., Bush, K. T., Steer, D. L., Stuart, R. O., Sakurai, H., Wachsman, W. and Nigam, S. K. (2001). Multiple fibroblast growth factors support growth of the ureteric bud but have different effects on branching morphogenesis. *Mech. Dev.* **109**, 123-135.

Schmahl, J., Kim, Y., Colvin, J. S., Ornitz, D. M. and Capel, B. (2004). Fgf9 induces proliferation and nuclear localization of FGFR2 in Sertoli precursors during male sex determination. *Development* **131**, 3627-3636.

Sekine, K., Ohuchi, H., Fujiwara, M., Yamasaki, M., Yoshizawa, T., Sato, T., Yagishita, N., Matsui, D., Koga, Y., Itoh, N. et al. (1999). Fgf10 is essential for limb and lung formation. *Nat. Genet.* **21**, 138-141.

Simian, M., Hirai, Y., Navre, M., Werb, Z., Lochter, A. and Bissell, M. J. (2001). The interplay of matrix metalloproteinases, morphogens and growth factors is necessary for branching of mammary epithelial cells. *Development* **128**, 3117-3131.

Sun, X., Mariani, F. V. and Martin, G. R. (2002). Functions of FGF signalling from the apical ectodermal ridge in limb development. *Nature* **418**, 501-508.

Tsang, M. and Dawid, I. B. (2004). Promotion and attenuation of FGF signaling through the Ras-MAPK pathway. *Sci STKE* **2004**, pe17.

Uhlmann, E., Peyman, A., Ryte, A., Schmidt, A. and Buddecke, E. (2000). Use of minimally modified antisense oligonucleotides for specific inhibition of gene expression. *Meth. Enzymol.* **313**, 268-284.

Weaver, M., Dunn, N. R. and Hogan, B. L. (2000). Bmp4 and Fgf10 play opposing roles during lung bud morphogenesis. *Development* **127**, 2695-2704.

Wells, A. and Marti, U. (2002). Signalling shortcuts: cell-surface receptors in the nucleus? *Nat. Rev. Mol. Cell. Biol.* **3**, 697-702.

Yeh, B. K., Igarashi, M., Eliseenkova, A. V., Plotnikov, A. N., Sher, I., Ron, D., Aaronson, S. A. and Mohammadi, M. (2003). Structural basis by which alternative splicing confers specificity in fibroblast growth factor receptors. *Proc. Natl. Acad. Sci. USA* **100**, 2266-2271.

Zang, X. P., Lerner, M. R., Dunn, S. T., Brackett, D. J. and Pento, J. T. (2003). Antisense KGFR oligonucleotide inhibition of KGF-induced motility in breast cancer cells. *Anticancer Res.* **23**, 4913-4919.

Zhou, M., Sutliff, R. L., Paul, R. J., Lorenz, J. N., Hoying, J. B., Haudenschild, C. C., Yin, M., Coffin, J. D., Kong, L., Kranias, E. G. et al. (1998). Fibroblast growth factor 2 control of vascular tone. *Nat. Med.* **4**, 201-207.